Activation of long non-coding RNA NEAT1 leads to survival advantage of multiple myeloma cells by supporting a positive regulatory loop with DNA repair proteins

Activation of lncRNA NEAT1 leads to survival advantage of multiple myeloma cells by supporting a positive regulatory loop with DNA repair proteins

Elisa Taiana[1,2]*, Cecilia Bandini[3,4], Vanessa Katia Favasuli[1,2], Domenica Ronchetti[1,2], Ilaria Silvestris[1,2], Noemi Puccio[1,2], Katia Todoerti[1], Silvia Erratico[5,6], Domenica Giannandrea[7], Niccolò Bolli[1,2], Nicola Amodio[8], Alessia Ciarrocchi[9], Raffaella Chiaramonte[7], Yvan Torrente[6], Roberto Piva[3,4], Antonino Neri[1,2]*.

[1]Hematology, Fondazione Cà Granda IRCCS Policlinico, 20122 Milan, Italy

[2]Department of Oncology and Hemato-oncology, University of Milan, Italy20122 Milan,

[3]Department of Molecular Biotechnology and Health Sciences, University of Turin, 10126 Turin, Italy

[4]Città Della Salute e della Scienza Hospital, 10126 Turin, Italy

[5]Novystem Spa, Milan, Italy

[6]Stem Cell Laboratory, Department of Pathophysiology and Transplantation, University of Milan, Centro Dino Ferrari, Unit of Neurology, Fondazione Cà Granda IRCCS Policlinico, 20122 Milan, Italy

[7]Department of Health Sciences, University of Milan, 20142 Milan, Italy

[8]Department of Experimental and Clinical Medicine, Magna Graecia University of Catanzaro, 88100 Catanzaro, Italy

[9]Laboratory of Translational Research, Azienda Unità Sanitaria Locale-IRCCS Reggio Emilia, 42123 Reggio Emilia, Italy

*Authors to whom correspondence should be addressed:
elisa.taiana@unimi.it;
antonino.neri@ausl.re.it; Present address: Scientific directorate, Azienda Unità Sanitaria Locale-IRCCS Reggio Emilia, 42123, Italy

CONFLICT OF INTEREST

The authors declare that they have no conflict of interest.

ABSTRACT

Malignant plasma cells of patients affected by multiple myeloma (MM) express at high levels the nuclear long non-coding RNAs NEAT1, which represents the core structural component of paraspeckle organelles (PS). We previously demonstrated that NEAT1 silencing negatively impacts proliferation and viability of MM cells, both *in vitro* and *in vivo*, highlighting its pivotal role in regulating the Homologous Recombination pathway. This study suggested NEAT1 involvement in virtually all DNA repair mechanisms, through the significant increase of PS number within cells and the activation of a molecular axis including the two fundamental kinase proteins ATM and DNA-PKcs, and the direct targets pRPA32 and pCHK2. Furthermore, we found that NEAT1 overexpression is associated with oncogenic and pro-survival advantages in MM cells exposed to nutrient starvation or hypoxic microenvironment, which are stressful conditions often associated with more aggressive disease phases. Overall, we provided novel important insights into NEAT1 role in supporting MM cells adaptation to stressful conditions by improving the maintenance of DNA integrity. Taken together, our results suggest that NEAT1, and probably PS organelles, could represent a potential therapeutic target for MM treatment.

INTRODUCTION

Multiple myeloma (MM) is a malignant proliferation of bone marrow plasma cells (PCs) characterized by different clinical course and a highly heterogeneous genetic background with both structural chromosomal alterations and specific genes mutations [1,2].

Over the past decade, a causal relationship between deregulation of long non-coding RNAs (lncRNA) and the pathogenesis of human cancers, including MM, has emerged by different functional studies [3-6]. LncRNAs participate in several biological processes, such as transcriptional gene regulation, genomic integrity maintenance, cell differentiation and development [7].

We have identified the nuclear paraspeckle assembly transcript 1 (NEAT1) as one of the abundantly expressed lncRNAs in malignant PCs compared to its normal counterpart [6,8,9] consistently with its high expression levels in many solid tumors [10]. NEAT1 is a mono-exonic lncRNA, transcribed from the Multiple Endocrine Neoplasia (MEN) type I locus, localized on the chromosome 11q13 [11]. Two different variants of NEAT1 exist and share identical 5' terminus: NEAT1_1, a shorter polyadenylated isoform of 3.7 kb, and NEAT1_2, a longer isoform of 22.7 kb, lacking the polyA tail [12]. NEAT1 has been demonstrated to be a fundamental structural component of nuclear paraspeckles (PSs), which are irregularly shaped compartments of the nuclear interchromatin space, considered as membraneless lncRNA-directed nuclear bodies involved in stress response [9,13]. Consistently with this function, we highlighted a pivotal role for NEAT1 in the maintenance of DNA integrity, through the regulation of the homologous recombination (HR) pathway, by demonstrating that NEAT1 depletion led to a significant downregulation of genes and active fractions of proteins involved in initial and crucial steps of the HR pathway [6]. Moreover, our research group demonstrated that NEAT1 silencing negatively regulates proliferation and viability of MM cells, both *in vitro* and *in vivo* [6].

Despite the growing amount of data obtained by loss-of-function approaches, concerning the role of NEAT1 in the DNA damage repair (DDR) system and maintenance of genome integrity [6,13-15], the biological scenario underlying MM cells following NEAT1 overexpression remains virtually absent.

In recent years, different approaches of CRISPR/Cas9 system have been explored to induce gene activation [16] or gene repression [17]. In particular, the CRISPR/Cas9 Synergistic Activation Mediator (SAM) system is a cutting-edge technique that uses MS2 bacteriophage coat proteins combined with p65 and HSF1 to para-physiologically induce the transcription of target genes without altering the DNA sequence [18].

Using this approach, here, we investigated the functional role of NEAT1 transactivation in human MM cell lines (HMCLs). In particular, we established a relevant role for NEAT1 in DNA repair molecular mechanisms through the up-regulation of the two fundamental kinases, namely ATM and DNA-PKcs. Furthermore, our data strongly indicate NEAT1 involvement in conferring survival advantage to MM cells exposed to stressful conditions such as nutrient starvation or hypoxic microenvironment, thus suggesting that the specific targeting of the PSs backbone could be a promising novel strategy in MM treatment.

MATERIALS AND METHODS

Full details of lentivirus production and *in vitro* transduction, plasmid constructs and cloning of sgRNAs, quantitative real-time PCR, colony-forming assay, cell cycle analysis and apoptosis, immunofluorescence, RNA FISH, gymnotic delivery, inhibitors and antibiotics, proteomic assays are provided in Supplementary Methods.

MM Cell Lines and Drugs

AMO-1 was kindly provided by Dr. C. Driessen (University of Tubingen, Germany). LP1, MM1.S, OPM2, and NCI-H929 were purchased from DSMZ, which certified authentication performed by short tandem repeat DNA typing. All HMCLs were immediately frozen and used from the original stock within 6 months. HMCLs were cultured in RPMI-1640 medium (Gibco®, Life Technologies, Carlsbad, CA, USA) supplemented with 10% fetal bovine serum (FBS), 100 U/ml penicillin, and 100 mg/ml streptomycin (Gibco®) at 37°C in 5% CO_2 atmosphere, and tested for mycoplasma contamination.

Hypoxia and HIF-1α stabilization

Hypoxia was induced by placing the cells for 24/48 h into a modular incubator chamber (Billups Rothenberg Inc., Del Mar, CA, USA) flushed with a mixture of 1% O_2, 5% CO_2 and 94%N_2 at 37°C. To achieve oxygen-independent HIF-1α stabilization, cells were exposed to 100 μM $CoCl_2$ for 24 h [19].

Statistical analysis

Statistical significance of differences observed was determined by Student t test analysis; differences were considered significant when P value was <.05 (*), <.01 (**), or <.001 (***). All statistical analyses were performed using the Prism 5.0 software (GraphPad Software, Inc.)

RESULTS

NEAT1 transactivation increases the amount of paraspeckles in MM cells

To activate the endogenous expression of NEAT1 in MM cells, we took advantage of the CRISPR/Cas9 SAM genome editing system. We first engineered the AMO-1 cell line to stably express the components of the CRISPR activation system (dCas9/ MS2-p65-HSF1) (Supplementary Fig. 1a). Then, AMO-1 cells were individually transduced with three sgRNAs targeting the NEAT1 promoter or a scramble sgRNA (Supplementary Table 1 and Supplementary Fig. 1b). RT-qPCR of selected cells demonstrated that two out of three NEAT1 targeting sgRNAs induced significant NEAT1 transactivation (AMO-$1^{N\#5}$ and AMO-$1^{N\#8}$ cells) compared to the scramble condition (AMO-1^{SCR} cells) (Fig. 1a). Specific RNA FISH confirmed the sustained NEAT1 expression levels obtained in both targeted cell lines (Supplementary Fig. 1c).

Since NEAT1 has been demonstrated to be the fundamental structural component of nuclear PSs [9], we evaluated whether the increased NEAT1 transcription affects the expression of the essential PS proteins (PSPs). Interestingly, NEAT1 overexpression was associated with a significant increase of NONO and SFPQ protein expression in AMO-$1^{N\#5}$ and AMO-$1^{N\#8}$ cells (Fig. 1b). Similarly, we detected also the overexpression of the FUS protein, whose prionlike low complexity domain is required for the organization of a microscopically visible mature PS [20] (Fig. 1b). However, PSPs mRNA expression levels were not significantly modulated in AMO-$1^{N\#5}$ and AMO-$1^{N\#8}$ cells (Supplementary Fig. 1d). This prompted us to investigate the role of NEAT1 in the regulation of PSPs stability. To address this issue, we monitored the time course of NONO and FUS disappearance in the presence of the protein synthesis inhibitor cycloheximide (CHX). Our analysis indicated that the degradation rate of NONO and FUS was significantly slower in NEAT1-transactivated AMO-1 cells (Fig. 1c). Furthermore, neither NONO nor FUS completely disappeared even after long CHX exposure (Supplementary Fig. 1e).

Finally, we evaluated if the stabilization of PSPs induced by NEAT1 activation was associated with a positive modulation of PSs size and distribution in AMO-1 cells. Our analyses of

AMO-1$^{N\#5}$ and AMO-1$^{N\#8}$ cells by confocal microscopy revealed that NEAT1 and NONO co-localized in PS organelles, whose number and size were increased compared to AMO-1^{SCR} cells (Supplementary Fig. 2).

NEAT1 transactivation provides a survival advantage to MM cells cultured under stressful conditions

To evaluate whether MM cells could benefit from a survival advantage upon NEAT1 transactivation, we monitored the growth rate and viability of AMO-1$^{N\#5}$, AMO-1$^{N\#8}$, and AMO-1^{SCR} cells in physiological and stressful conditions. In the first case, AMO-1$^{N\#5}$, AMO-1$^{N\#8}$ cell lines showed cell growth and viability similar to AMO-1^{SCR} cells (Supplementary Fig. 3a and 3b). We confirmed the absence of significant modulation in the cell cycle phase distributions and in the apoptotic rate by flow cytometric analysis (Supplementary Fig. 3c and 3d). Consistently, we did not observe any change also in the clonogenic potential (Supplementary Fig. 3e).

Based on NEAT1 involvement during cellular stress response [9,13,21], we assessed the relevance of NEAT1 transactivation in stressful conditions, such as FBS starvation or hypoxia.

First, we assessed NEAT1 expression modulation under stressful condition. Both total NEAT1 and NEAT1_2 isoform expression levels of AMO-1$^{N\#5}$, AMO-1$^{N\#8}$, and AMO-1^{SCR} cells cultured for 48 h at 1% FBS condition resulted significantly up-regulated in comparison with the relative counterpart maintained in 10% FBS (Fig. 2a), confirming that both variants are induced under stressful conditions. Interestingly, FBS starvation increased the fraction of the NEAT1_2 isoform (Fig. 2b), which is known to be the fundamental structural scaffold for the biogenesis of PS organelles. Confocal microscopy analysis revealed that FBS starvation not only induces NEAT1 expression but also NONO protein expression, leading to an increase in the number of PSs identifiable by co-localized signals (Fig. 2c). Similar results were obtained by growing MM cells in hypoxic microenvironment, resulting in a significant up-regulation of both NEAT1 isoforms (Supplementary Fig. 4a), particularly of the fraction of NEAT1_2 long variant (Supplementary Fig.

4b). Moreover, in line with results obtained with serum starvation, the up-regulation of NEAT1 upon hypoxia positively correlated with the increase of NONO expression and the number and size of PS organelles (Supplementary Fig. 4c).

From a biological point of view, upon FBS starvation NEAT1-activated cells showed a significant higher viability as compared to AMO-1^{SCR} cells (Fig. 3a). This finding is supported also by a reduced plasmatic membrane integrity observed in AMO-1^{SCR} compared to AMO-1$^{N\#5}$ and AMO-1$^{N\#8}$ (Supplementary Fig. 5a) and by a cell cycle analysis that showed a higher percentage of cells distributed in sub G0/G1 phase (Fig. 3b and Supplementary Fig. 5b). Additionally, the presence of a significant higher percentage of apoptotic cells (Fig. 3c) in AMO-1^{SCR} cells suggests also an anti-apoptotic role of NEAT1. Moreover, NEAT1 transactivation significantly increased the clonogenic potential of MM cells cultured in the same condition (Fig. 3d). In detail, sustained NEAT1 expression increased the number of colonies that also resulted to be larger, more structured and compact (Fig. 3e and Supplementary Fig. 5c).

In agreement with these biological data, in condition of serum starvation, the active fraction of ERK1/2 and AKT proteins were up-regulated in NEAT1 transactivated cells, displaying a higher increase in the more aggressive AMO-1$^{N\#8}$ compared to AMO-1^{SCR} cells (Fig. 3f).

Finally, we could observe a greater viability and modulation of cell cycle phase distribution also in NEAT1 transactivated AMO-1 cells maintained in hypoxic condition (Supplementary Fig. 5d, 5e, and 5f).

NEAT1 transactivation leads to the phosphorylation of RPA32 and CHK2 through a molecular mechanism dependent on ATM and DNA-PKcs

We previously demonstrated NEAT1 involvement in the DDR system [6]. With the aim of dissecting the molecular mechanisms associating NEAT1 with DNA repair processes, we investigated RPA32 expression following NEAT1 transactivation.

Specifically, WB and confocal microscopy analysis showed an up-regulation of pRPA32 levels in NEAT1 transactivated cells compared to AMO-1^{SCR} cells (Fig. 4a and Supplementary Fig. 6a), whereas RPA32 total form remained unchanged at both protein (Fig. 4a) and mRNA level (Supplementary Fig. 6b). Furthermore, AMO-1$^{N\#5}$ and AMO-1$^{N\#8}$ cells displayed increased levels of the active fraction of CHK2 (Fig. 4b), another important player of DDR system, whereas no significant modulation of pCHK1 was detected (Fig. 4b).

To shed light on the possible mechanism by which NEAT1 leads to an increase of activated RPA32, we evaluated the expression levels of the three main kinase proteins responsible for its phosphorylation, i.e. ATM, ATR and DNA-PK [22]. Our results showed that NEAT1 induction did not associate with significant modulations of ATM, ATR and PRKDC mRNA levels, ruling out a possible role of NEAT1 in the transcriptional regulation of these proteins (Supplementary Fig. 6c). We also confirmed at protein level that NEAT1 transactivation did not induce a significant modulation of ATR and its activated form (Fig. 4c), in line with the absence of modulation of its direct target pCHK1. Conversely, ATM protein levels increased in AMO-1$^{N\#5}$ and AMO-1$^{N\#8}$ cells with respect to AMO-1^{SCR} cells (Fig. 4c), in agreement with the increased pCHK2 and pRPA32 expression levels. Furthermore, also the catalytic subunit of DNA-PK (DNA-PKcs) showed a significant increase in NEAT1 activated cells compared to AMO1^{SCR} cells (Fig. 4c), data also confirmed by immunofluorescence (Supplementary Fig. 6d).

Overall, our data are consistent with a signaling pathway downstream NEAT1 triggered through the increase of ATM and DNA-PKcs protein levels, which in turn trigger RPA32 and CHK2 activation via phosphorylation.

NEAT1-mediated activation of RPA32 is enhanced upon FBS starvation and hypoxic condition

The evidence that FBS starvation positively modulates NEAT1 expression (Fig. 2) prompted us to verify the outcome of FBS starvation on the molecular axis "NEAT1-pRPA32". At this purpose, we compared AMO-1^{SAM} cells cultured upon FBS starving and physiological conditions.

Interestingly, confocal microscopy analyses demonstrated increased levels of both DNA-PKcs and its target pRPA32 in AMO-1^{SCR} cells cultured in FBS starving condition (Fig. 5a), in line with a possible relationship between NEAT1/PSs expression and DNA-PKcs activity. Of note, AMO-1$^{N\#5}$ and AMO-1$^{N\#8}$ cells exposed to 1% FBS further increase the expression levels of pRPA32, DNA-PKcs and ATM compared to AMO-1^{SCR}, confirming the role of NEAT1 in triggering the mechanism that brings to RPA32 phosphorylation (Fig. 5b).

Similarly, hypoxia, another condition that increases NEAT1 expression (Supplementary Fig. 4), determines DNA-PKcs levels higher than those observed in normoxic condition, above all in both AMO-1$^{N\#5}$ and AMO-1$^{N\#8}$ cells compared to AMO-1^{SCR} cells (Fig. 5c).

To further validate the effects of hypoxic stress, we investigated AMO-1^{SAM} cells upon $CoCl_2$ treatment that chemically stabilize HIF-1 transcription factor. Also in this case, we detected the overexpression of NEAT1 and NONO in association with the increase of both DNA-PKcs and pRPA32 protein levels (Supplementary Fig. 7a). In agreement with the effects of hypoxic and FBS starving conditions, the up-regulation of DNA-PKcs upon $CoCl_2$ treatment further increased in NEAT1 transactivated cells (Supplementary Fig. 7b), which, at the same time, showed a higher viability and a lower percentage of apoptotic cells than AMO-1^{SCR} cells (Supplementary Fig. 7c and 7d).

With the aim of validating our data, we extended the study to other three HMCLs (OPM2, MM1.S and LP1), based on the hypothesis that FBS starving condition could induce NEAT1 expression. As expected, serum starvation induced NEAT1 expression in all HMCLs tested (Supplementary Fig. 8a), and we detected an increase of the NEAT1_2 variant contribution with respect to total NEAT1 expression (Supplementary Fig. 8b). Moreover, WB analysis demonstrated an increase in the pRPA32 amount in FBS starved cells compared to cells maintained at normal

FBS condition (Supplementary Fig. 8c). In agreement with our model, DNA-PKcs and ATM protein levels increased in FBS starved cells (Supplementary Fig. 8c). Finally, also FUS protein resulted overexpressed, likely to enhance PSs assembling (Supplementary Fig. 8c).

The long NEAT1_2 variant is essential for the regulation of the DNA-PK, ATM/pRPA32 axis

To confirm NEAT1 fundamental role in the regulation of DNA-PKcs and ATM and the consequent RPA32 activation, we evaluated the expression levels of both kinase proteins in AMO-1 and LP1 cells specifically silenced for NEAT1. As expected, the down-regulation of both NEAT1 isoforms, obtained through the gymnotic delivery of the antisense LNA-gapmeR g#N1_E (Fig. 6a), results in the reduction of the pRPA32 protein levels (Fig. 6b). In addition, g#N1_E-silenced cells showed a significant reduction of both DNA-PKcs and ATM protein levels, thus confirming a pivotal role of NEAT1 in the regulation of pRPA32 expression through a mechanism DNA-PK and ATM-mediated (Fig. 6b).

Finally, to evaluate if the molecular effect of NEAT1 silencing was orchestrated mainly by the short and more abundant isoform of NEAT1 or by the long NEAT1_2 variant, we silenced AMO-1 and LP1 cells with an LNA-gapmeR specific for the NEAT1_2 isoform (g#N1_G). Of note, the silencing of NEAT1_2 was sufficient to determine the down-regulation of pRPA32 and of both DNA-PKcs, and ATM (Fig. 6b).

The NEAT1/ pRPA32 positive axis is responsible for survival advantages of MM cells

Finally, we investigated whether the pro-survival effect observed in NEAT1 transactivated cells cultured in non-physiological conditions, such as FBS starvation, was supported, at least in part, by the novel identified NEAT1-orchestrated molecular axis.

Hence, we chemically inhibited ATM and DNA-PK activity in AMO-1^{SAM} cells cultured in FBS starving conditions, and evaluated the biological impact. As expected, in FBS starvation we found that pRPA32 levels in AMO-$1^{N\#8}$ were higher than in AMO-1^{SCR} cells; however, the

inhibition of both ATM and DNA-PK kinases led to the impairment of RPA32 phosphorylation in both cell lines (Supplementary Fig. 9a). In line with our hypothesis, both ATM and DNA-PK inhibition resulted in a significant reduction of cell viability in AMO-1^{SCR} and AMO-$1^{N\#8}$ starved cells, even more evident upon simultaneous inhibition of ATM and DNA-PK activities (Fig. 7a). Furthermore, FBS starved cells clearly showed alteration of cell membrane integrity and membrane blebbing in AMO-1^{SCR} cells compared to NEAT1 transactivated cells. These characteristics are typical of apoptotic cells, in line with the higher level of mortality (Fig. 7b and Supplementary Fig. 9b). Interestingly, the same morphological changes were detectable in FBS starved-AMO-1^{SAM} cells upon the simultaneous inhibition of ATM and DNA-PK (Fig. 7b and Supplementary Fig. 9b), in agreement with the significant decrease of cell viability. Moreover, the inhibition of ATM and DNA-PK was associated with a massive cytoplasmic vacuolization, more pronounced upon simultaneous inhibition of both protein kinases, suggesting a suffering cell phenotype (Fig. 7b and Supplementary Fig. 9b).

Notably, NEAT1 silencing in NCI-H929 cell line and in CD138+ purified primary PCs also led to cytoplasmic vacuolization, even if at a lesser extent (Fig. 7c), suggesting that the molecular and biological effect observed upon NEAT1 silencing could be the result, at least in part, of the reduced activity of the NEAT1/ pRPA32 axis.

DISCUSSION

We previously reported that NEAT1 expression in purified PCs from MM patients is significantly higher than in normal counterpart and that NEAT1 silencing negatively regulates proliferation and viability of MM cells, both *in vitro* and *in vivo*, by affecting the DNA damage cellular response [6].

PSs are dynamic compartment in the nuclear interchromatin space. They respond to different stimuli among which DNA damage. These pieces of evidence together with the function of NEAT1 in PSs assembly, prompted us to investigate the mechanism underlying the pro-tumoral effect of

NEAT1 by studying how NEAT1 overexpression observed in MM can influence the activity of PSs during DDR.

To mimic the effect of NEAT1 overexpression in MM, we get advantage of two NEAT1 transactivated MM clones obtained by using the innovative CRISPR-Cas9 SAM gain of function approach [17].

First, we demonstrated that the para-physiological activation of NEAT1 is associated with a significant increase of the levels of essential PSPs such as NONO, SFPQ, and FUS. In details, NEAT1 extends the half-life of these three PSPs, thereby rising their availability within MM cells. Moreover, confocal microscopy analysis clearly showed that overexpressed NEAT1 and NONO co-localize in PS organelles, whose number significantly augmented in NEAT1 transactivated cells, confirming previous data reporting that NEAT1 transcription was coupled with PSs assembling [23]. Importantly, the three PSPs are involved in virtually all DNA repair mechanisms (see review [9]). In particular, NONO/SFPQ creates a heterodimer that can associate with the major proteins of the non-homologous end-joining (NHEJ) thus promoting their activity; SFPQ was reported to be essential for HR pathway activation, by promoting the formation of D-loops during the homologous pairing recombination. Moreover, SFPQ can act as both activator and inhibitor of RAD51, exerting a tight regulation of HR pathway. FUS plays a fundamental role in both double strand breaks (DSBs), where its depletion leads to HR and NHEJ impairment, and single strand brakes (SSBs) repair, since it is recruited by PARP1 to promote the recruitment of base excision repair (BER) proteins at the DNA damage site. Overall, this evidence, together with the fact that NEAT1 can be a direct target of the TP53 transcription factor [14], support the hypothesis of a functional contribution of NEAT1, and likely of PSs, in DDR pathway.

Since PSs are important in the cell response to different stimuli including stressful conditions, such as nutrient starvation and hypoxia, we investigated the role of NEAT1 in stressful culturing conditions. Our investigation established that NEAT1 overexpression is crucial to sustain the growth and the survival potential of MM cells when maintained in non-physiological culturing

conditions. Indeed, hypoxia and nutrient starvation further induce NEAT1 expression in AMO-1^{SAM} clones, which positively correlates with an increase of both PSs number within cells and cell survival. In agreement with our data, NEAT1 up-regulation under hypoxic condition has been already reported in hepatocellular carcinoma and non-small cell lung cancer, where NEAT1 represents a target of the HIF-1 or HIF-2 transcription factors, respectively; also in this context, NEAT1 overexpression provides the cell with pro-survival and oncogenic properties [24,25]. In MM cells as well, we found that the transactivation of NEAT1 not only guarantees pro-survival advantages, but also increases their oncogenic potential, as demonstrated by the higher colony-forming potential obtained upon FBS starving conditions, as well as the more structured colonies organization.

In line with the role of NEAT1 in supporting MM cell survival during FBS starvation, we observed the activation of ERK and AKT-mediated cell survival pathways in NEAT1 transactivated cells cultured.

Overall, these findings suggest that NEAT1 targeting may have great translational relevance since both serum starvation and hypoxia are typical stressful conditions for tumor cells *in vivo* and are often associated with more aggressive tumor stages and mechanisms of chemo-resistance.

Based on the functional impact of NEAT1 both in the DDR pathways and in the growth and survival of MM cells when cultured in non-physiological conditions, we hypothesized that NEAT1 transactivation may induce survival advantage in MM cells under stressful conditions by improving DNA repair mechanisms. In agreement with this theory, we demonstrated that, along with the stabilization of NONO, SFPQ, and FUS, NEAT1 transactivation is associated with the overexpression of other two crucial proteins of the DDR system, DNA-PKcs and ATM, thus leading to the activation of their target proteins RPA32 and CHK2 (Fig 4 and Supplementary Fig. 6). We validated the positive association between NEAT1 transcription levels and the expression of the DDR proteins in NEAT1 transactivated cells under stressful condition; in fact, we showed that, similarly to NEAT1 expression levels, also DDR protein levels further increase in non-

physiological culture conditions (Fig 5 and Supplementary Fig. 7). Finally, transactivated NEAT1 cells in stressful conditions also exhibit significantly greater viability (Supplementary Fig. 7), indicating a pro-survival and pro-oncogenic role of NEAT1-mediated axis in MM.

The molecular circuit driven by NEAT1 and its crucial role for MM cell survival under stressful condition was further validated by different approaches. First, we demonstrated that the chemical inhibition of ATM and/or DNA-PK in NEAT1 transactivated AMO-1^{SAM} cells under stressful conditions significantly decreases cell viability and leads to cell morphological changes characterized by a massive cytoplasmic vacuolization (Fig. 7 and supplementary Fig 9). In agreement with our observations, this peculiar phenotype preceding cell death has been reported in osteosarcoma cells, upon ATR inhibition [26].

To validate the obtained results, we verified NEAT1-mediated molecular axis in other HMCLs, thus excluding a cell line specific effect. Indeed, serum starving conditions induce the up-regulation of NEAT1, DNA-PK, ATM, and pRPA32 in OPM2, LP1, and MM1.S HMCLs (Supplementary Fig. 8). Furthermore, NEAT1 silencing in AMO-1 and LP1 negatively affects the expression levels of both DNA-PKcs and ATM protein kinases, and of the active amount of RPA32 (Fig. 6). Of note, NEAT1 silencing in NCI-H929 cell line and in CD138+ purified primary PCs leads to a pattern of cytoplasmic vacuolization similar to the phenotype obtained with the chemical inhibition of ATM and/or DNA-PK (Fig. 7c), suggesting that the molecular and biological effect highlighted upon NEAT1 silencing could be the result, at least in part, of the reduced activity of DNA-PK and ATM on pRPA32.

Taken together, our data indicated that the up-regulation of ATM, DNA-PKcs, and pRPA32 could be considered a general molecular response of MM cells to NEAT1 induction, which, in turn, could represent a survival advantage for MM cell facing adverse conditions.

Interestingly, our results pointed out an important role for the long NEAT1_2 variant under stressful conditions; in fact, both in AMO-1^{SAM} clones and in all HMCLs tested, FBS starvation or hypoxia significantly increase the NEAT1_2 percentage respect to total NEAT1 expression. This

finding suggests that non-physiological conditions may shift NEAT1 transcription towards the long NEAT1_2 isoform, likely to assemble the PSs needed to counteract the stressful condition. In accordance with this evidence, the specific targeting of the long NEAT1_2 variant negatively affects the expression levels of both DNA-PKcs and ATM protein kinases, and of the active amount of RPA32, suggesting that the structural scaffold of PSs, and maybe PSs themselves, should be considered master regulators of DNA damage response in MM cells.

In conclusion, our study attributes a crucial role to NEAT1 overexpression in MM; pathological NEAT1 expression and the consequent deregulation of PS organelles availability, could represent an Achilles' heel for MM PCs survival and strongly suggest that NEAT1 and PSs targeting could be considered a novel promising strategy for innovative anti-MM therapies.

Acknowledgements

This work was financially supported by grants from Associazione Italiana Ricerca sul Cancro (AIRC) to AN (IG16722 and IG24365), to RC (IG20614), to RP (IG21585), and to NA (IG24449). NB is funded by the European Research Council under the European Union's Horizon 2020 research and innovation program (grant agreement no. 817997). YT acknowledges support by "Piattaforme cellulari per la Ricerca e lo Sviluppo di Terapie Avanzate in Life Science" - Fondo Europeo di Sviluppo Regionale 2014-2020. POR FESR 2014-2020. CB received two-years AIRC fellowship "Angela e Luciano Cenino" (id.24140); VKF and DG received a fellowship by the PhD program in Experimental Medicine of Milano University. We thank Prof. Gariboldi M. and Dr. Marras M. for making the modular incubator chamber available.

AUTHOR CONTRIBUTIONS

ET, CB, VKF, IS, NP, and KT performed experiments and analyzed the data; ET, DG and IS performed cytofluorimetric experiments; ET and SE performed confocal analysis; NB, NA, AC, RC, YT, and RP provided critical evaluation of experimental data and of the manuscript. ET, AN, and DR conceived the study and wrote the manuscript.

COMPETING INTERESTS

The authors declare that they have no conflict of interest.

REFERENCES

1. Bolli N, Biancon G, Moarii M, Gimondi S, Li Y, de Philippis C, *et al.* Analysis of the genomic landscape of multiple myeloma highlights novel prognostic markers and disease subgroups. *Leukemia* 2018 Dec; 32(12): 2604-2616.
2. Munshi NC, Anderson KC. New strategies in the treatment of multiple myeloma. *Clinical cancer research : an official journal of the American Association for Cancer Research* 2013 Jul 1; 19(13): 3337-3344.
3. Amodio N, Stamato MA, Juli G, Morelli E, Fulciniti M, Manzoni M, *et al.* Drugging the lncRNA MALAT1 via LNA gapmeR ASO inhibits gene expression of proteasome subunits and triggers anti-multiple myeloma activity. *Leukemia* 2018 Sep; 32(9): 1948-1957.
4. Huarte M. The emerging role of lncRNAs in cancer. *Nature medicine* 2015 Nov; 21(11): 1253-1261.
5. Morelli E, Gulla A, Rocca R, Federico C, Raimondi L, Malvestiti S, *et al.* The Non-Coding RNA Landscape of Plasma Cell Dyscrasias. *Cancers* 2020 Jan 30; 12(2).
6. Taiana E, Favasuli V, Ronchetti D, Todoerti K, Pelizzoni F, Manzoni M, *et al.* Long non-coding RNA NEAT1 targeting impairs the DNA repair machinery and triggers anti-tumor activity in multiple myeloma. *Leukemia* 2020 Jan; 34(1): 234-244.

7. Wang KC, Chang HY. Molecular mechanisms of long noncoding RNAs. *Molecular cell* 2011 Sep 16; 43(6): 904-914.
8. Taiana E, Ronchetti D, Favasuli V, Todoerti K, Manzoni M, Amodio N, *et al.* Long non-coding RNA NEAT1 shows high expression unrelated to molecular features and clinical outcome in multiple myeloma. *Haematologica* 2019 Feb; 104(2): e72-e76.
9. Taiana E, Ronchetti D, Todoerti K, Nobili L, Tassone P, Amodio N, *et al.* LncRNA NEAT1 in Paraspeckles: A Structural Scaffold for Cellular DNA Damage Response Systems? *Non-coding RNA* 2020 Jul 1; 6(3).
10. Yu X, Li Z, Zheng H, Chan MT, Wu WK. NEAT1: A novel cancer-related long non-coding RNA. *Cell proliferation* 2017 Apr; 50(2).
11. Guru SC, Agarwal SK, Manickam P, Olufemi SE, Crabtree JS, Weisemann JM, *et al.* A transcript map for the 2.8-Mb region containing the multiple endocrine neoplasia type 1 locus. *Genome research* 1997 Jul; 7(7): 725-735.
12. Naganuma T, Nakagawa S, Tanigawa A, Sasaki YF, Goshima N, Hirose T. Alternative 3'-end processing of long noncoding RNA initiates construction of nuclear paraspeckles. *The EMBO journal* 2012 Oct 17; 31(20): 4020-4034.
13. Adriaens C, Marine JC. NEAT1-containing paraspeckles: Central hubs in stress response and tumor formation. *Cell cycle* 2017 Jan 17; 16(2): 137-138.
14. Adriaens C, Standaert L, Barra J, Latil M, Verfaillie A, Kalev P, *et al.* p53 induces formation of NEAT1 lncRNA-containing paraspeckles that modulate replication stress response and chemosensitivity. *Nature medicine* 2016 Aug; 22(8): 861-868.
15. Blume CJ, Hotz-Wagenblatt A, Hullein J, Sellner L, Jethwa A, Stolz T, *et al.* p53-dependent non-coding RNA networks in chronic lymphocytic leukemia. *Leukemia* 2015 Oct; 29(10): 2015-2023.
16. Maeder ML, Linder SJ, Cascio VM, Fu Y, Ho QH, Joung JK. CRISPR RNA-guided activation of endogenous human genes. *Nature methods* 2013 Oct; 10(10): 977-979.

17. Qi LS, Larson MH, Gilbert LA, Doudna JA, Weissman JS, Arkin AP, *et al.* Repurposing CRISPR as an RNA-guided platform for sequence-specific control of gene expression. *Cell* 2013 Feb 28; 152(5): 1173-1183.

18. Konermann S, Brigham MD, Trevino AE, Joung J, Abudayyeh OO, Barcena C, *et al.* Genome-scale transcriptional activation by an engineered CRISPR-Cas9 complex. *Nature* 2015 Jan 29; 517(7536): 583-588.

19. Yuan Y, Hilliard G, Ferguson T, Millhorn DE. Cobalt inhibits the interaction between hypoxia-inducible factor-alpha and von Hippel-Lindau protein by direct binding to hypoxia-inducible factor-alpha. *The Journal of biological chemistry* 2003 May 2; 278(18): 15911-15916.

20. Fox AH, Nakagawa S, Hirose T, Bond CS. Paraspeckles: Where Long Noncoding RNA Meets Phase Separation. *Trends in biochemical sciences* 2018 Feb; 43(2): 124-135.

21. McCluggage F, Fox AH. Paraspeckle nuclear condensates: Global sensors of cell stress? *BioEssays : news and reviews in molecular, cellular and developmental biology* 2021 May; 43(5): e2000245.

22. Byrne BM, Oakley GG. Replication protein A, the laxative that keeps DNA regular: The importance of RPA phosphorylation in maintaining genome stability. *Seminars in cell & developmental biology* 2019 Feb; 86: 112-120.

23. Mao YS, Sunwoo H, Zhang B, Spector DL. Direct visualization of the co-transcriptional assembly of a nuclear body by noncoding RNAs. *Nature cell biology* 2011 Jan; 13(1): 95-101.

24. Kong X, Zhao Y, Li X, Tao Z, Hou M, Ma H. Overexpression of HIF-2alpha-Dependent NEAT1 Promotes the Progression of Non-Small Cell Lung Cancer through miR-101-3p/SOX9/Wnt/beta-Catenin Signal Pathway. *Cellular physiology and biochemistry : international journal of experimental cellular physiology, biochemistry, and pharmacology* 2019; 52(3): 368-381.

25. Zhang X, Kang Z, Xie X, Qiao W, Zhang L, Gong Z, *et al.* Silencing of HIF-1alpha inhibited the expression of lncRNA NEAT1 to suppress development of hepatocellular carcinoma under hypoxia. *American journal of translational research* 2020; 12(7): 3871-3883.

26. Li X, Dean DC, Cote GM, Zou L, Hornicek FJ, Yu S, *et al.* Inhibition of ATR-Chk1 signaling blocks DNA double-strand-break repair and induces cytoplasmic vacuolization in metastatic osteosarcoma. *Therapeutic advances in medical oncology* 2020; 12: 1758835920956900.

LEGEND TO FIGURES

Figure 1. NEAT1 transactivation associates with PSPs increased expression levels. a Analyses of total NEAT1 and NEAT1_2 expression levels in NEAT1 transactivated AMO-$1^{N\#5}$ and AMO-$1^{N\#8}$ cell lines with respect to AMO-1^{SCR} cells, based on the qRT-PCR approach described in the schematic representation. NEAT1 expression was expressed as $2^{-\Delta\Delta Ct}$ relative to the scramble condition. *p<0.05 *vs*. SCR; ***p < 0.001 *vs*. SCR. **b** WB of NONO, SFPQ, and FUS in AMO-1^{SAM} cells. GAPDH protein expression was included for protein loading normalization. **c** Effect of NEAT1 transactivation in the presence of the protein synthesis inhibitor CHX (100 μM) on the decay of NONO and FUS protein levels in AMO-1^{SCR} and AMO-$1^{N\#8}$ cells at indicated time point. Actin protein expression was included for protein loading normalization. The densitometric analysis of immunoreactive bands is reported with respect to SCR condition in WB experiments.

Figure 2. FBS starvation up-regulates NEAT1 and increases PSs number. a qRT-PCR analyses of total NEAT1 and NEAT1_2 expression in AMO-1^{SAM} cells maintained for 48 h in physiological FBS culturing condition (10% FBS) and in FBS starving medium. NEAT1 expression was expressed as $2^{-\Delta Ct}$. **b** Percentage of NEAT1_2 variant contribution respect to total NEAT1 expression in AMO-1^{SAM} cells maintained for 48 h in physiological FBS culturing condition (10% FBS) and in FBS starving medium. **c** Confocal microscopy results of NEAT1 specific RNA-FISH and NONO IF in AMO-1 cells cultured for 48 h in physiological FBS culturing condition (10% FBS) and in FBS starving medium (scale bar 5μm).

Figure 3. NEAT1 transactivation improves MM cells survival and oncogenic potential in non-physiological culturing conditions. a Growth curve and viability of AMO-1^{SAM} cells cultured for 72 h in FBS starving condition. *p<0.05 *vs*. SCR. **b** Cell cycle analysis by PI staining performed in AMO-1^{SAM} cells after 48 h of culture in FBS starving condition; specific histograms representing the percentage of cells in sub G0/G1 are also shown. *p<0.05 vs. SCR. **c** Flow cytometric analysis of apoptosis in AMO-1^{SCR}, AMO-$1^{N\#5}$ and AMO-$1^{N\#8}$ cultured for 72 h in FBS starving condition.

d Colony formation assay performed on AMO-1^{SAM} cultured for 31 days in FBS starving condition; representative pictures of colonies distribution at day 31 are also shown. **e** Representative pictures of colonies formed in AMO-1^{SCR}, AMO-1$^{N\#5}$ and AMO-1$^{N\#8}$ 24 days after seeding (10x magnification). **f** WB of pERK 1/2, ERK 1/2, pAKT, and AKT in AMO-1^{SAM} cells after 48 h of culture in FBS starving conditions. GAPDH protein expression was included for protein loading normalization. Percentage of pERK1/2 and pAKT with respect to total ERK1/2 and AKT (both normalized for GAPDH expression) is also shown.

Figure 4. NEAT1 transactivation up-regulates proteins involved in DNA repair process. a WB of pRPA32 and RPA32 in AMO-1^{SAM} cells. **b** WB of pCHK2, CHK2, pCHK1, and CHK1 in AMO-1^{SAM} cells **c** WB of pATR, ATR, pATM, ATM, and DNA-PKcs in AMO-1^{SAM}. The densitometric analysis of DNA-PKcs immunoreactive bands is reported with respect to SCR condition. Furthermore, the percentage of activated fraction of all proteins with respect to relative total amount (both normalized for GAPDH expression) is reported.

Figure 5. MM cells under stressful conditions overexpress NEAT1 and other proteins involved in DNA repair process. a Confocal microscopy results of DNA-PKcs and pRPA32 specific IF in AMO-1 cells cultured in physiological FBS culturing condition (10% FBS) and in FBS starving medium (scale bar 20μm). **b** WB analysis of pRPA32, RPA32, DNA-PKcs and ATM in AMO-1^{SAM} cells after 48 h of culture in FBS starving condition. GAPDH protein expression was included for protein loading normalization. Percentage of pRPA32 with respect to total RPA32 (both normalized for GAPDH expression) is also shown. **c** WB analysis of DNA-PKcs in AMO-1^{SAM} cells after 48 h of culture in normoxic and hypoxic conditions. Actin protein expression was included for protein loading normalization. The densitometric analysis of immunoreactive bands is reported with respect to SCR condition.

Figure 6. NEAT1 silencing down-regulates proteins involved in DNA repair process. a Scheme of LNA-gapmeR localization on NEAT1 transcript; qRT-PCR analyses of NEAT1 expression

levels in AMO-1 and LP1 MM cell lines upon gymnotic delivery of g#N1_E or g#N1_G LNA-gapmeR. NEAT1 expression was expressed as $2^{-\Delta Ct}$. **b** WB analysis of pRPA32, RPA32, DNA-PKcs, and ATM in AMO-1 and LP1 cells after gymnotic delivery of NEAT1-targeting gapmeR (5 μM). GAPDH protein expression was included for protein loading normalization. The densitometric analysis of DNA-PKcs and ATM immunoreactive bands is reported with respect to SCR condition. Furthermore, the percentage of pRPA32 with respect to total RPA32 (both normalized for GAPDH expression) is also shown.

Figure 7. ATM and DNA-PK inhibitions abrogate NEAT1 pro survival advantages. a Viability of AMO-1^{SCR} and AMO-$1^{N\#8}$ cells after three days of culture in FBS starving condition, in the presence for the last 24 h of ATM and DNA-PK inhibitors, respectively KU-60019 and NU7026. **b** Optical microscopy results of May Grunwald-Giemsa (MGG) staining obtained in AMO-1^{SCR} and AMO-$1^{N\#8}$ cells after three days of culture in FBS starving condition, in the presence for the last 24 h of ATM and DNA-PK inhibitors. (100x magnification). **c** Optical microscopy results of May Grunwald-Giemsa (MGG) staining obtained in NCI-H929 and CD138+ MM primary cells after three days from the gymnotic delivery of NEAT1-targeting gapmeR (5 μM). (100x magnification).

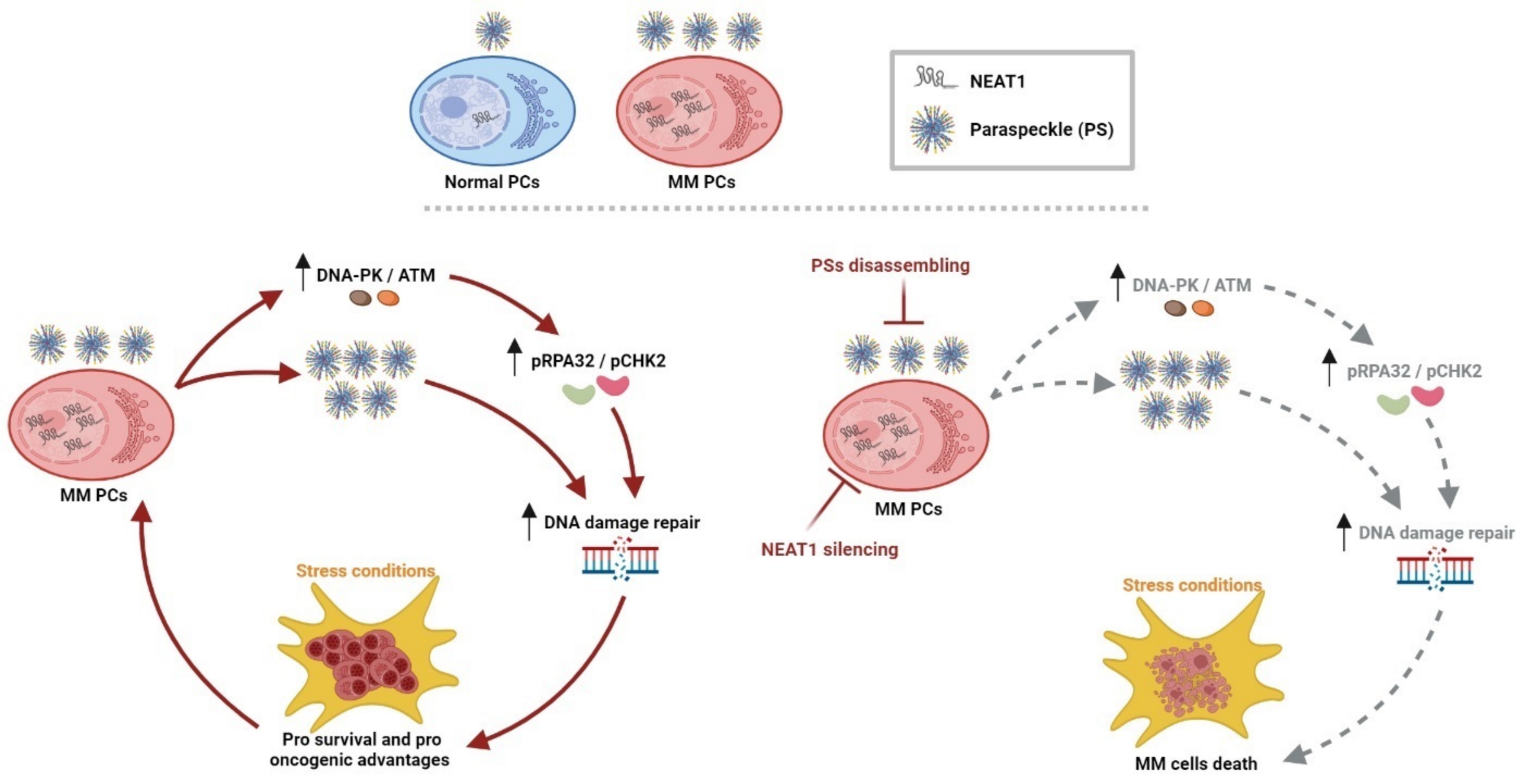
Normal PCs
MM PCs
NEAT1
Paraspeckle (PS)
DNA-PK / ATM
pRPA32 / pCHK2
MM PCs
DNA damage repair
Stress conditions
Pro survival and pro oncogenic advantages
PSs disassembling
NEAT1 silencing
DNA-PK / ATM
pRPA32 / pCHK2
MM PCs
DNA damage repair
Stress conditions
MM cells death

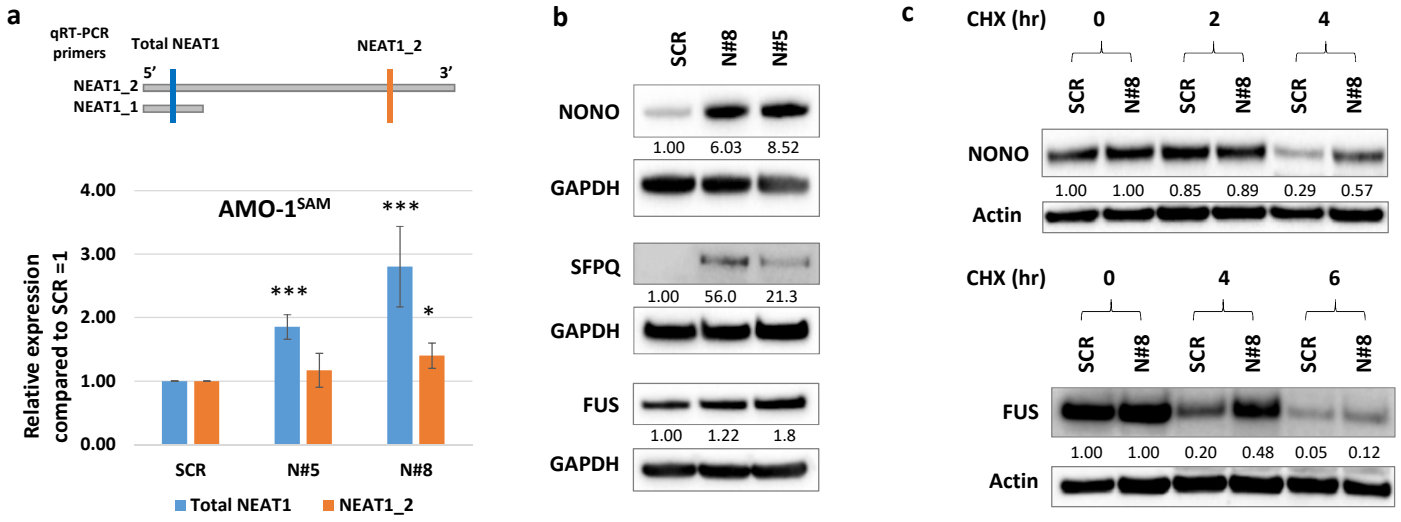
a
qRT-PCR primers
Total NEAT1
NEAT1_2
5'
3'
NEAT1_2
NEAT1_1
AMO-1SAM
Relative expression compared to SCR =1
4.00
3.00
2.00
1.00
0.00
***
***
*
SCR
N#5
N#8
Total NEAT1
NEAT1_2
b
SCR
N#8
N#5
NONO
1.00
6.03
8.52
GAPDH
SFPQ
1.00
56.0
21.3
GAPDH
FUS
1.00
1.22
1.8
GAPDH
c
CHX (hr)
0
2
4
SCR
N#8
SCR
N#8
SCR
N#8
NONO
1.00
1.00
0.85
0.89
0.29
0.57
Actin
CHX (hr)
0
4
6
SCR
N#8
SCR
N#8
SCR
N#8
FUS
1.00
1.00
0.20
0.48
0.05
0.12
Actin

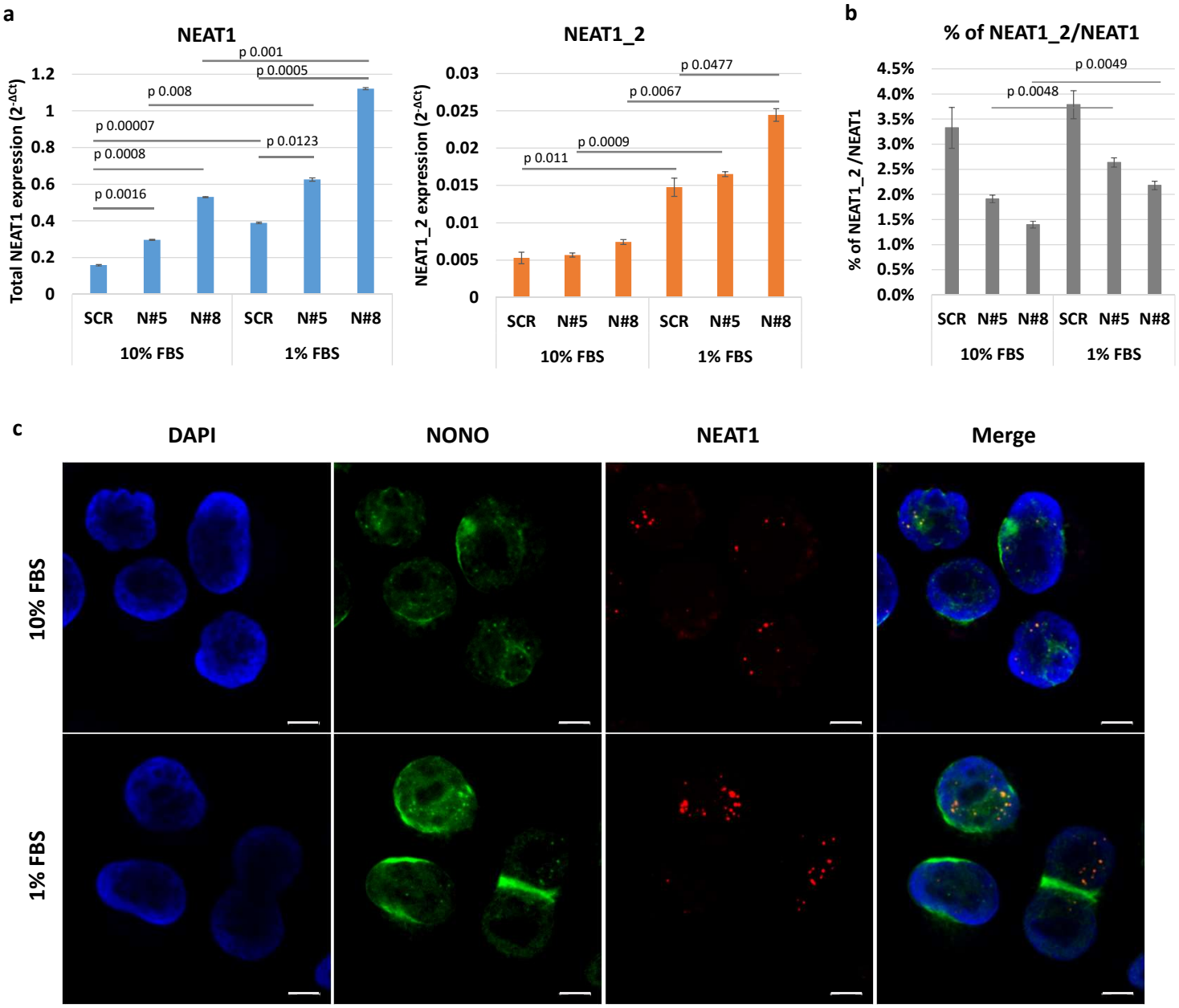
a
NEAT1
Total NEAT1 expression (2-ΔCt)
p 0.001
p 0.0005
p 0.008
p 0.00007
p 0.0123
p 0.0008
p 0.0016
SCR
N#5
N#8
SCR
N#5
N#8
10% FBS
1% FBS
NEAT1_2
NEAT1_2 expression (2-ΔCt)
p 0.0477
p 0.0067
p 0.0009
p 0.011
SCR
N#5
N#8
SCR
N#5
N#8
10% FBS
1% FBS
b
% of NEAT1_2/NEAT1
% of NEAT1_2 /NEAT1
p 0.0049
p 0.0048
SCR
N#5
N#8
SCR
N#5
N#8
10% FBS
1% FBS

c
DAPI
NONO
NEAT1
Merge
10% FBS
1% FBS

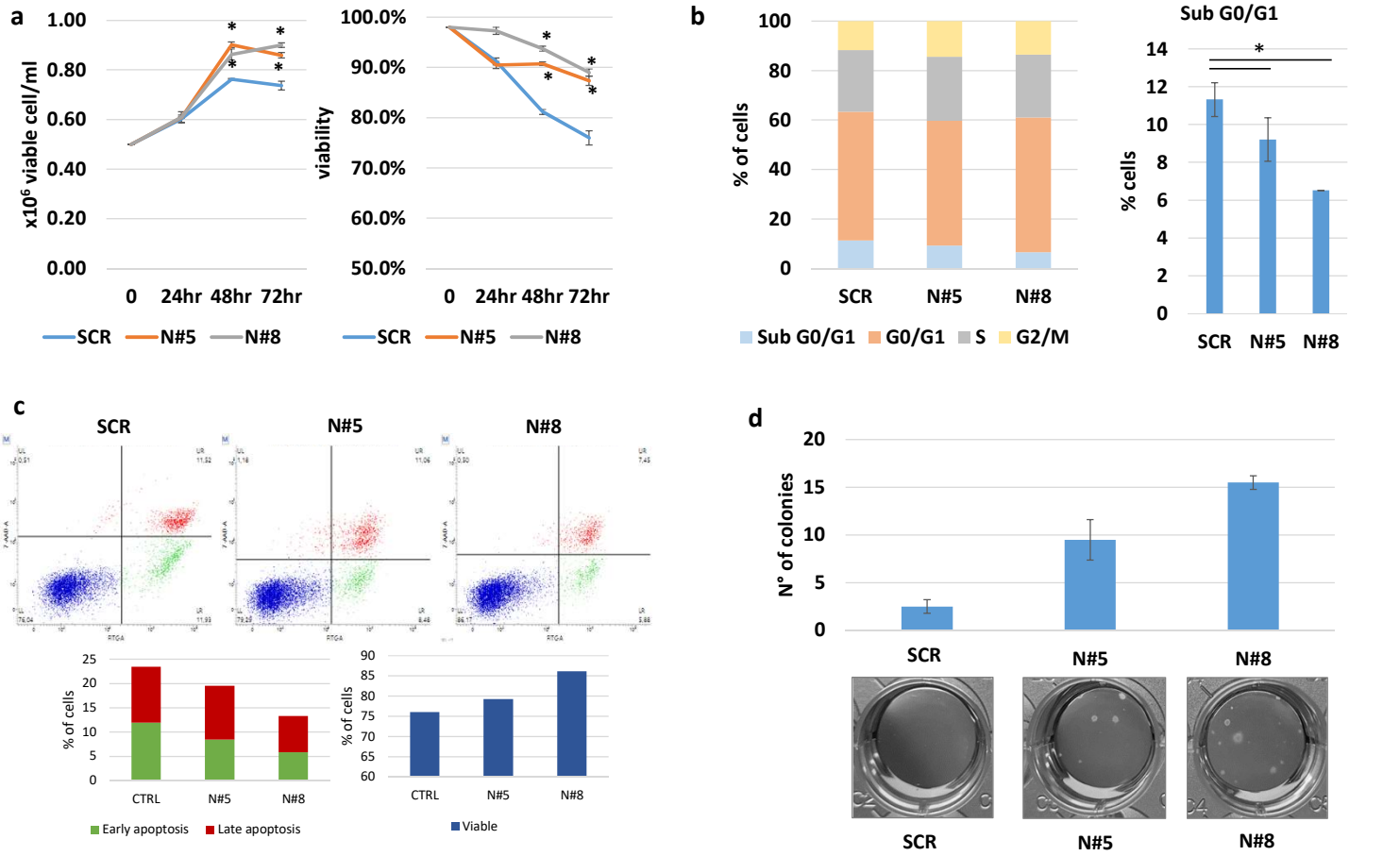
a
x10⁶ viable cell/ml
1.00
0.80
0.60
0.40
0.20
0.00
0
24hr
48hr
72hr
SCR
N#5
N#8
viability
100.0%
90.0%
80.0%
70.0%
60.0%
50.0%
b
% of cells
100
80
60
40
20
0
Sub G0/G1
G0/G1
S
G2/M
Sub G0/G1
% cells
14
12
10
8
6
4
2
0
c
SCR
N#5
N#8
% of cells
25
20
15
10
5
0
CTRL
Early apoptosis
Late apoptosis
90
85
80
75
70
65
60
Viable
d
N° of colonies
20
15
10
5
0
e
24 days
f
pERK1/2
ERK1/2 tot
pERK/ERKtot
0.62
0.75
1.05
GAPDH
pAKT
AKT tot
pAKT/AKTtot
0.99
0.91
2.13

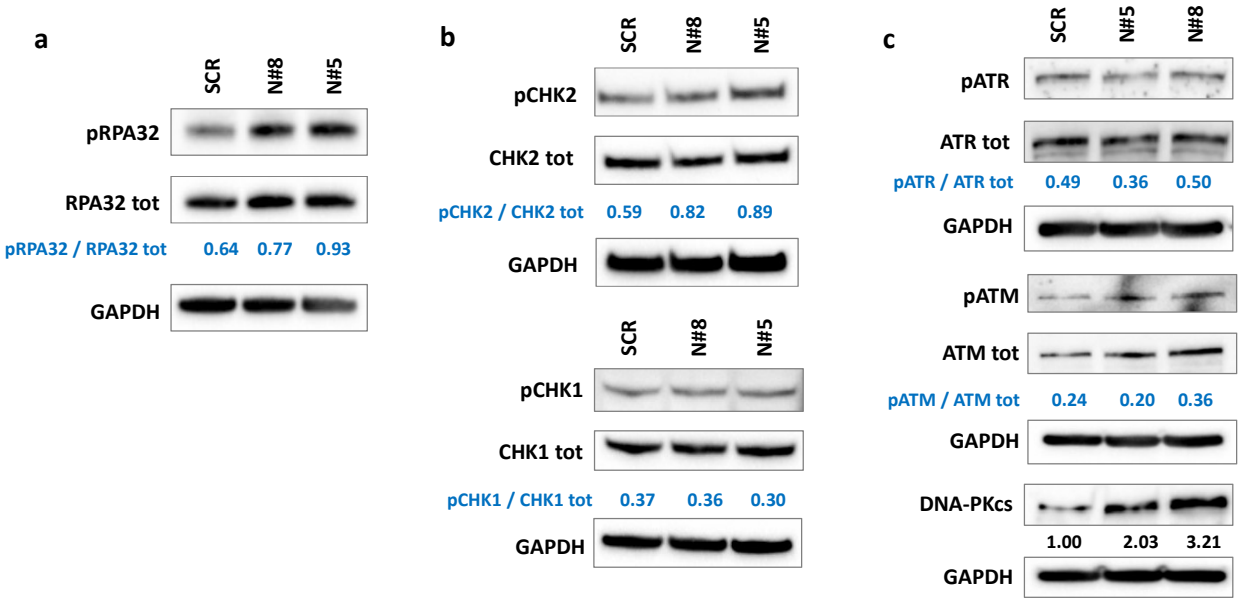
a
SCR
N#8
N#5
pRPA32
RPA32 tot
pRPA32 / RPA32 tot 0.64 0.77 0.93
GAPDH
b
SCR
N#8
N#5
pCHK2
CHK2 tot
pCHK2 / CHK2 tot 0.59 0.82 0.89
GAPDH
SCR
N#8
N#5
pCHK1
CHK1 tot
pCHK1 / CHK1 tot 0.37 0.36 0.30
GAPDH
c
SCR
N#5
N#8
pATR
ATR tot
pATR / ATR tot 0.49 0.36 0.50
GAPDH
pATM
ATM tot
pATM / ATM tot 0.24 0.20 0.36
GAPDH
DNA-PKcs
1.00 2.03 3.21
GAPDH

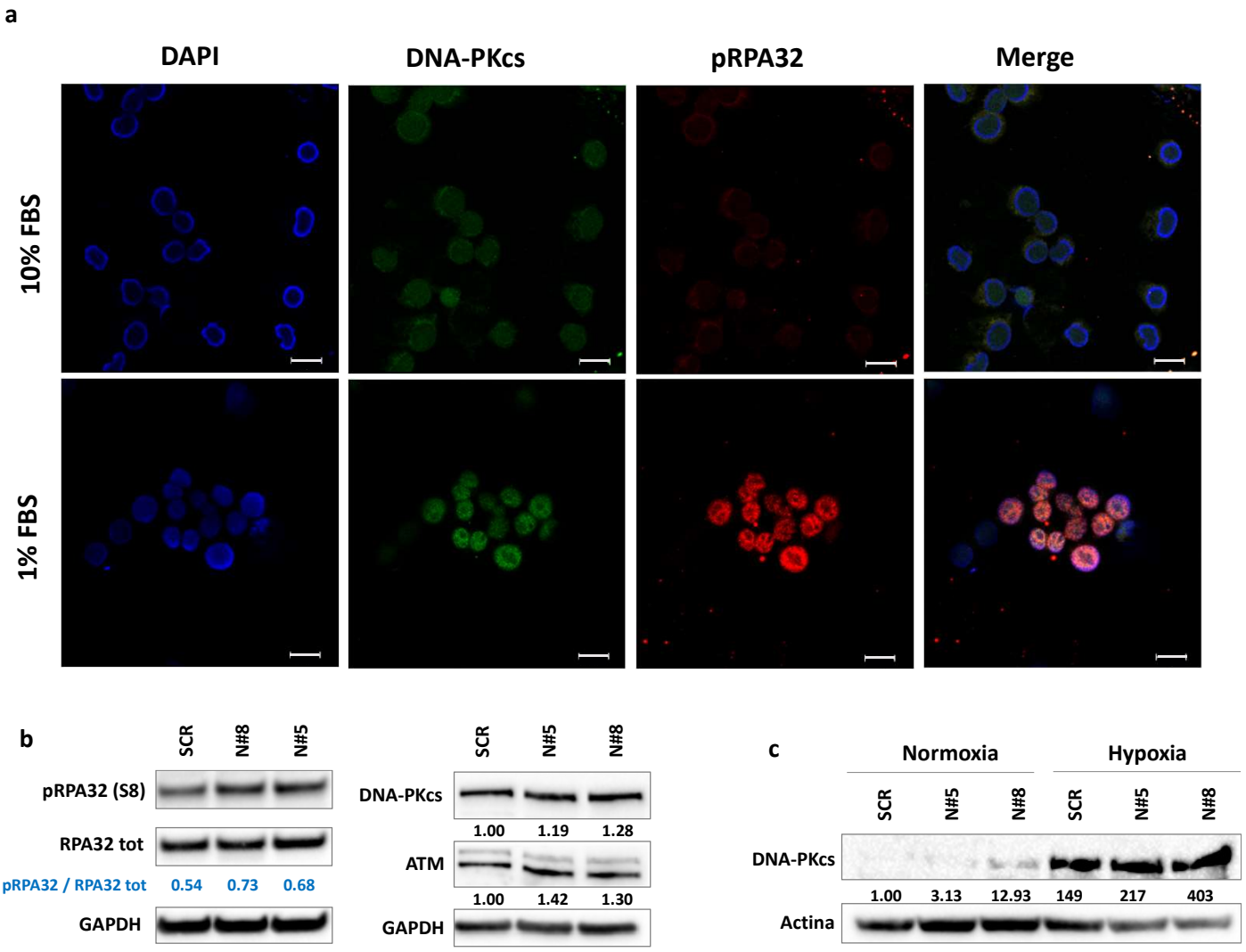
a
DAPI
DNA-PKcs
pRPA32
Merge
10% FBS
1% FBS
b
SCR
N#8
N#5
pRPA32 (S8)
RPA32 tot
pRPA32 / RPA32 tot
0.54
0.73
0.68
GAPDH
DNA-PKcs
1.00
1.19
1.28
ATM
1.00
1.42
1.30
GAPDH
c
Normoxia
Hypoxia
SCR
N#5
N#8
SCR
N#5
N#8
DNA-PKcs
1.00
3.13
12.93
149
217
403
Actina

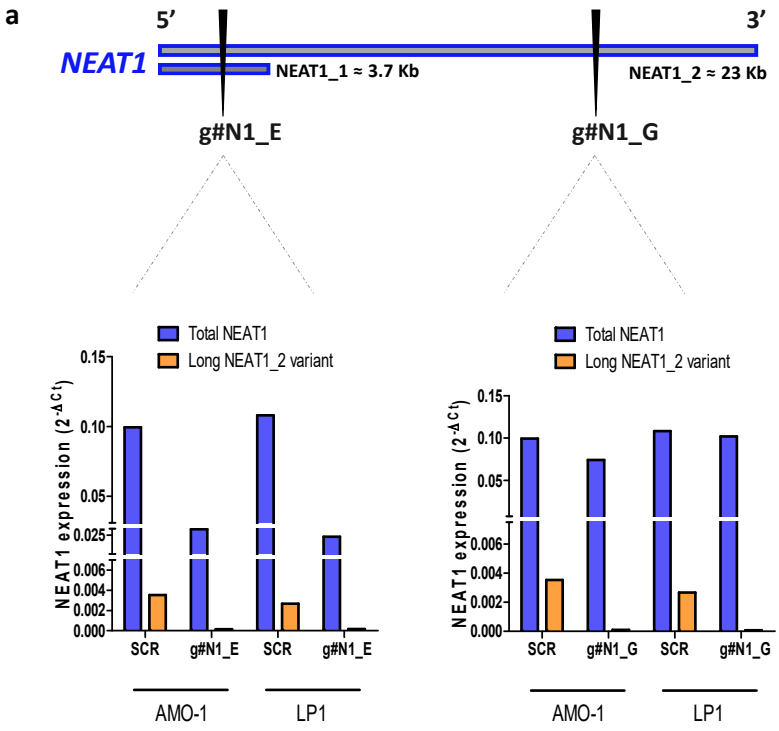
a
5'
3'
NEAT1
NEAT1_1 ≈ 3.7 Kb
NEAT1_2 ≈ 23 Kb
g#N1_E
g#N1_G
Total NEAT1
Long NEAT1_2 variant
NEAT1 expression (2-ΔCt)
0.15
0.10
0.05
0.025
0.006
0.004
0.002
0.000
SCR
g#N1_E
g#N1_G
AMO-1
LP1

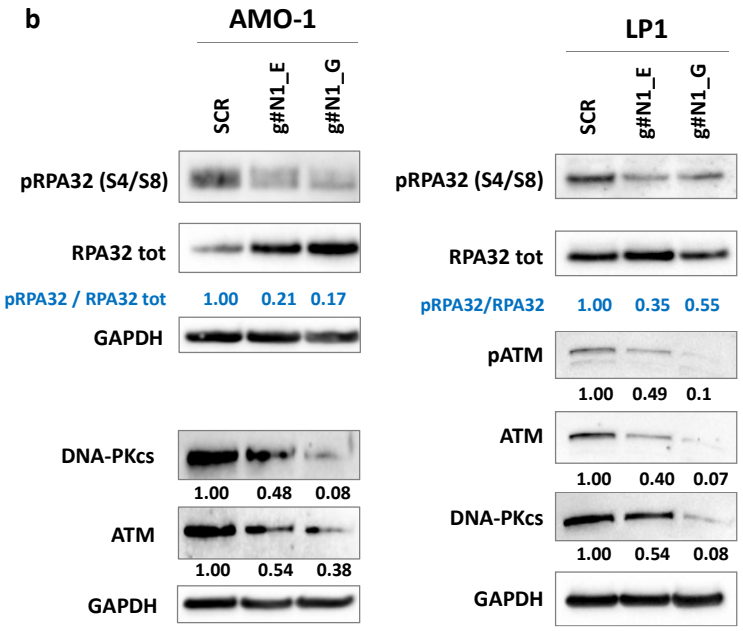
b
AMO-1
LP1
SCR
g#N1_E
g#N1_G
pRPA32 (S4/S8)
RPA32 tot
pRPA32 / RPA32 tot
1.00 0.21 0.17
GAPDH
DNA-PKcs
1.00 0.48 0.08
ATM
1.00 0.54 0.38
pRPA32/RPA32
1.00 0.35 0.55
pATM
1.00 0.49 0.1
1.00 0.40 0.07
1.00 0.54 0.08

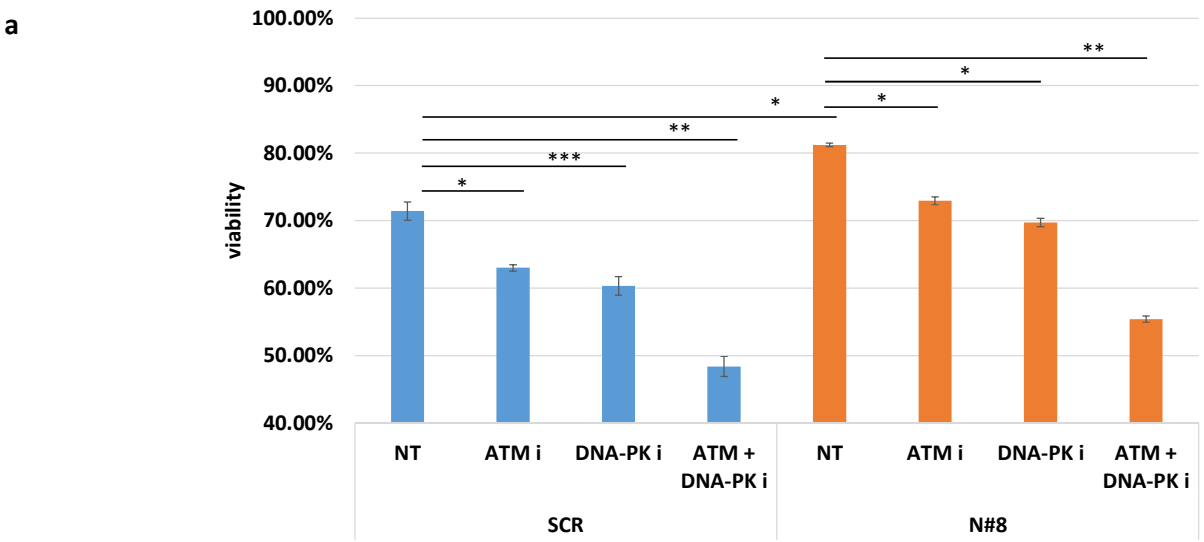
a
100.00%
90.00%
80.00%
70.00%
60.00%
50.00%
40.00%
viability
*
***
**
*
*
**
NT
ATM i
DNA-PK i
ATM + DNA-PK i
NT
ATM i
DNA-PK i
ATM + DNA-PK i
SCR
N#8

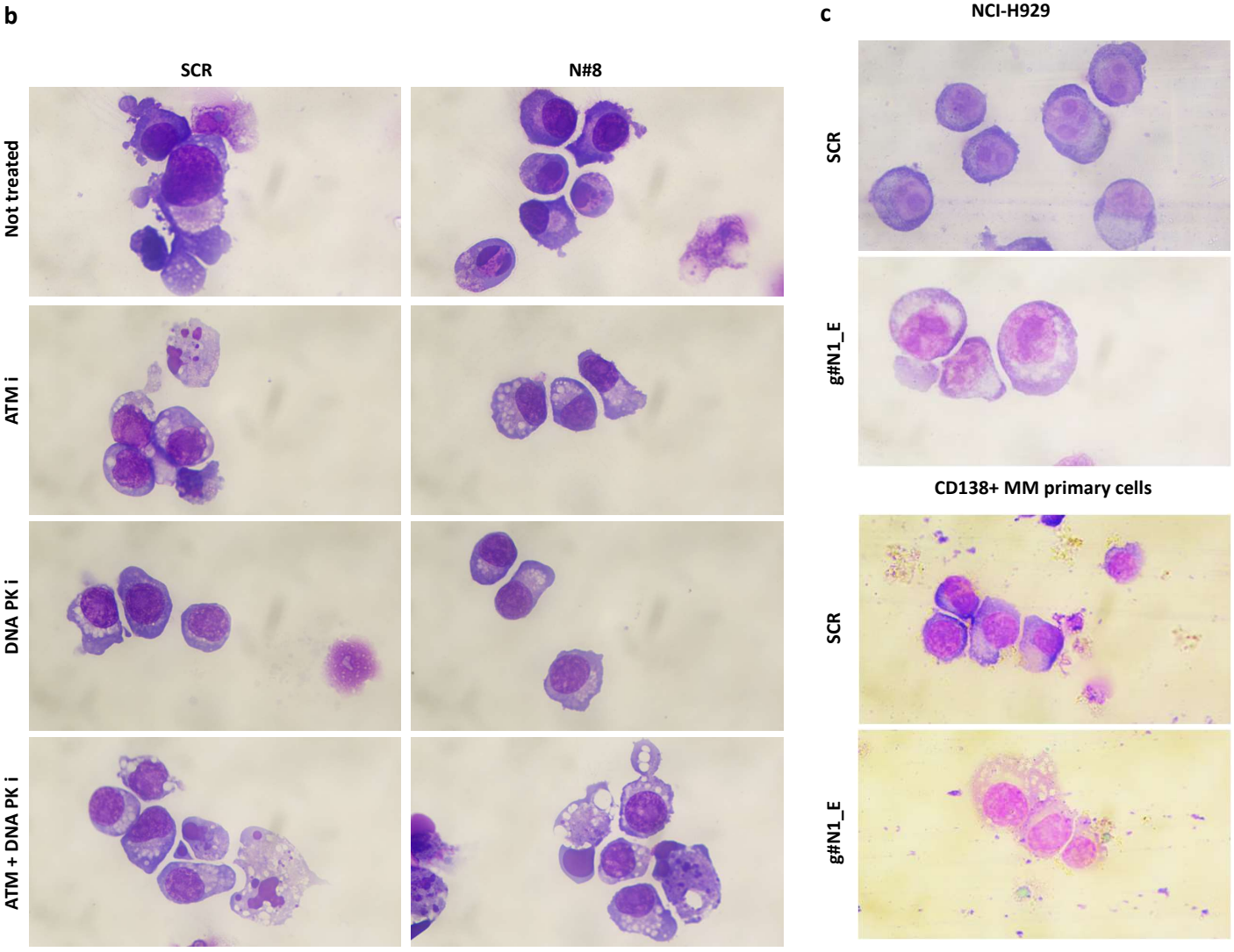
b
SCR
N#8
Not treated
ATM i
DNA PK i
ATM + DNA PK i
c
NCI-H929
SCR
g#N1_E
CD138+ MM primary cells
SCR
g#N1_E